International Journal of Development Mathematics Vol 3 Issue 3, 088–106

INTERNATIONAL JOURNAL OF DEVELOPMENT MATHEMATICS
ISSN: 3026-8656 (Print) | 3026-8699 (Online)
journal homepage: https://ijdm.org.ng/index.php/Journals

A Nonstandard Finite Difference Schemes for the Damped Harmonic Oscillator with Trigonometric Denominators: Convergence Analysis, Systematic Damping-Regime Validation, and Energy Conservation

Lukman O. Salaudeen[a*] **and Adesoji A. Obayomi**[b]

[a]Department of Mathematics,Federal University Oye-Ekiti, Nigeria.
[b]Department of Mathematics, Ekiti State University, Ado-Ekiti, Nigeria.

ARTICLE INFO

Article history:

Received 12 July 2026
Received in Revised 20 August 2026
Accepted 30 August 2026

Keywords

Nonstandard finite difference; harmonic oscillator; trigonometric interpolant; exponential denominator; damping; energy conservation; convergence.

MSC 2020 Subject classification: 65L06, 65L12, 65L20

Abstract

In this paper, we develop, analyse and extend a class of nonstandard finite difference (NSFD) schemes for the damped harmonic oscillator equation using a hybrid interpolant framework that incorporates trigonometric and exponential basis functions within a dynamically renormalised denominator structure. we develop three new numerical schemes **New-h**, **New-Sin**, and **New-Exp** characterised by the choice of a denominator function: $\psi = h$, $\psi = \sin(h)$, and $\psi = (e^{\gamma h} - 1)/\gamma$, respectively. Using the classical Henrici-Fatunla framework, detailed proofs of consistency, local stability and convergence of the proposed schemes are provided. We prove convergence using Gronwall error recursion, and rigorously analyse truncation errors to ensure *second-order* ($O(h^2)$) local consistency for each scheme; we analyse energy conservation to show that the New-Sin scheme outperforms the classical central difference method for undamped oscillators;

*Corresponding author Tel: +2348062163219
Email address: lukman.salaudeen@fuoye.edu.ng;
https://doi.org/10.62054/ijdm/0303.05

and we compare numerical results for four damping regimes and three stepsizes, resulting in maximum absolute errors that are two orders of magnitude smaller than those of the classical scheme.

1 Introduction

The harmonic oscillator is one of those problems that looks simple on paper, but in practice is inexhaustibly rich.

$$y'' + 2\varepsilon y' + y = 0, \tag{1}$$

Its equation of motion describes the motion of a mass-spring system, the current in an RLC circuit, the swing of a pendulum for small angles, and the response of countless physical systems to perturbation from equilibrium. The damping is controlled by the parameter $\varepsilon \geq 0$: $\varepsilon = 0$ gives undamped oscillations, $0 < \varepsilon < 1$ gives decaying oscillations, $\varepsilon = 1$ is critical damping, $\varepsilon > 1$ is over-damped. Since the exact solution is known analytically in all three regimes, equation (1) has become the standard benchmark for testing numerical integrators and a good one, because it involves the challenge of long-time accuracy and sensitivity to whether the scheme preserves important qualitative features such as decay rate, oscillation frequency, and energy budget.

The classical central finite difference (CFD) discretisation of (1) on a uniform grid $x_n = nh$ replaces derivatives by second order approximations, which yields a three-point recursion that is both consistent and convergent. But the classical scheme is well known to be weak, it does not preserve the qualitative structure of the continuous problem. For example, in the undamped case, the CFD scheme adds artificial numerical dissipation or growth depending on whether the product ωh (with $\omega = \sqrt{1-\varepsilon^2}$ being the angular frequency) is above or below a stability threshold. This implies that for the long-time integration of lightly damped oscillators, which is precisely the situation most relevant to engineering applications, the CFD method will eventually produce solutions that look qualitatively wrong, even when the pointwise errors appear to be small at early times. This is where non-standard finite difference (NSFD) methods come in. NSFD schemes, first introduced by Mickens (1993), replace the determinants in finite difference approximations by carefully chosen functions which satisfy local consistency but are designed to reproduce the qualitative behaviour of the continuous model. The main rules are (i) the first-order denominator $\mu(h)$ has to satisfy $\mu(h) \to h + O(h^2)$ as $h \to 0$; (ii) nonlinear terms have to be approximated non-locally with several mesh points and not just with one point; and (iii) the scheme has to preserve in discrete form as many of the conservation laws and qualitative properties of the original problem as possible (Anguelov and Lubuma, 2003; Mickens, 1993). Since the original work of Mickens, NSFD methods have been employed successfully on a variety of problems. Patidar (2016) reviewed comprehensively the NSFD developments for stability, consistency and applications in population dynamics, epidemiology and reaction-diffusion systems. NSFD schemes for stiff systems in chemical kinetics were developed by Zahra et al. (2019), who demonstrated that the nonstandard denominator can fully remove spurious oscillations. Dang and

Hoang (2020) used NSFD methods for a predator-prey system, showing that schemes constructed with Mickens' rules maintain positivity and boundedness unconditionally. In the special case of the oscillator, Zibaei and Namjoo (2014) designed elementary stable NSFD integrators for the nonlinear oscillator, and Wang et al. (2015) proved the construction of energy-preserving NSFD schemes for Hamiltonian ODEs by suitable choice of the nonlocal approximation. Zahra et al. (2019) extended the NSFD framework to fractional-order oscillators, demonstrating that the concept of denominator renormalization naturally carries over to the Caputo derivative setting. Obayomi et al. (2024) proposed three new NSFD schemes New-h, New-Sin and New-Exp for the equation (1) based on a hybrid trigonometric-exponential interpolant. In that paper, the new schemes were shown to be consistent, stable and convergent with convergence proofs adapted from Henrici (1962) and Fatunla (2014) and were shown numerically to outperform the Mickens (1993) NSFD scheme on four test problems. But the paper also raised many important questions.

This paper fills these gaps. We place the new schemes in a unified mathematical framework, extend the convergence proofs to include bounds on the truncation error, and provide a detailed numerical study that quantifies the advantages of the new schemes more precisely than previously established. We also present two new phase portraits and energy evolution analyzes that illustrate the qualitative superiority of the New-Sin scheme over the CFD method and the original Mickens (1993) scheme in the undamped and lightly damped cases. In particular, our contributions are: Self-contained presentation of the three new NSFD schemes in a unified notation; Full Taylor-expansion truncation error analysis establishing *second-order* ($O(h^2)$) local consistency; Principled denominator selection: $\psi^2 = 4\sin^2(h/2)$, $\mu = \sin(h)$ uniquely determined by the discrete dispersion relation of the ODE, with no free parameters; Phase-plane analysis confirms geometric fidelity of solution trajectories; Energy conservation study by using five integration methods; Sensitivity study of the step size and quantification of the convergence rate for six step sizes; Study of the damping regime for undamped, lightly damped, moderately damped and near-critically damped oscillators.

2 Mathematical Background

2.1 The Damped Harmonic Oscillator

We look at the following initial value problem.

$$y'' + 2\varepsilon y' + y = 0, \quad y(0) = y_0, \quad y'(0) = y_0', \quad x \in [0, T], \tag{2}$$

Here, $\varepsilon \geq 0$ is the dimensionless damping coefficient. The exact solution depends on the type of damping:

Under-damped ($\varepsilon < 1$)**:** $\omega_d = \sqrt{1-\varepsilon^2}$,

$$y(x) = e^{-\varepsilon x}(A\cos\omega_d x + B\sin\omega_d x)\,, \tag{3}$$

with $A = y_0$, $B = (y_0' + \varepsilon y_0)/\omega_d$.

Critically damped ($\varepsilon = 1$)**:** $y(x) = (A + Bx)e^{-x}$, with $A = y_0$, $B = y_0' + y_0$.

Over-damped ($\varepsilon > 1$)**:** $\omega_h = \sqrt{\varepsilon^2 - 1}$,

$$y(x) = e^{-\varepsilon x}(A\cosh\omega_h x + B\sinh\omega_h x)\,. \tag{4}$$

When there is no damping ($\varepsilon = 0$), the total mechanical energy $\mathcal{E}(x) = \frac{1}{2}[y'(x)]^2 + \frac{1}{2}y(x)^2$ is conserved: $\mathcal{E}(x) = \mathcal{E}(0)$ for all $x \geq 0$.

2.2 Nonstandard Finite Difference Rules

Suppose $\{x_n\}_{n=0}^N$ is a uniform grid with step size $h > 0$, where $x_n = nh$. The fundamental NSFD rules from Mickens (1993) and Anguelov and Lubuma (2003) are:

$$y' \approx \frac{y_{n+1} - y_n}{\mu(h)}, \quad \mu(h) \to h + O(h^2), \tag{5}$$

$$y' \approx \frac{y_{n+1} - \alpha(h)y_n}{\mu(h)}, \quad \alpha(h) \to 1, \tag{6}$$

$$y'' \approx \frac{y_{n+1} - 2y_n + y_{n-1}}{\psi^2(h)}, \quad \psi^2(h) \to h^2 + O(h^n), n > 2. \tag{7}$$

The choice of denominator functions is crucial for the qualitative behavior of the resulting scheme. This paper uses three denominator functions: paper are:

$$\mu_h = h \quad \text{(standard, New-h)}, \tag{8}$$

$$\mu_s = \sin(h) \quad \text{(trigonometric, New-Sin)}, \tag{9}$$

$$\mu_e = \frac{e^{\gamma h} - 1}{\gamma}, \gamma \in \mathbb{R} \setminus \{0\} \quad \text{(exponential, New-Exp)}. \tag{10}$$

Each satisfies $\mu(h) \to h + O(h^2)$ as $h \to 0$, as required by Mickens' Rule 1.

3 Derivation of the New Schemes

3.1 Hybrid Interpolation Function

We begin deriving our scheme by choosing an interpolation function that reflects the main features of the exact solution:

$$y(x) = a_0 + e^{\beta x} + a_1 x + a_2 \sin(\alpha x^2 + k), \tag{11}$$

where $a_0, a_1, a_2, \beta, \alpha, k$ are real parameters. This interpolant combines a polynomial component (capturing linear drift), an exponential component (capturing growth/decay), and a sinusoidal chirp component (capturing oscillatory behaviour with varying frequency). This interpolant's hybrid nature motivates the derivation below. In general the parameters α, β, k are free parameters. For the damped harmonic oscillator the physically motivated constraint is $\beta = -\varepsilon$ matching the real part of the characteristic root. Values $\beta > 0$ lead to an exponentially growing component which is not consistent with the decaying true solution and can destabilize the scheme. For the chirp part: the usual default is $k = 0$; α should be chosen such that the instantaneous frequency $2\alpha x_n \approx \omega_d$ at the mesh point

of interest, but this match is only local. Importantly, as demonstrated by the Taylor analysis in Section **??**, $E_n/P_n = h^2 + O(h^4)$, so the chirp correction only enters at the order $O(h^4)$ in the local truncation error. The main accuracy advantage of the scheme over classical FD is due to the choice of denominator $\mu = \sin(h)$ and not the interpolant parameters. For any fixed $\gamma > 0$ we have $\mu(h, \gamma) \to h$ in the exponential denominator. Thus, all variants are consistent, with γ only influencing the error constant.

Differentiating (11):

$$y' = \beta e^{\beta x} + a_1 + 2\alpha a_2 x \cos(\alpha x^2 + k), \tag{12}$$
$$y'' = \beta^2 e^{\beta x} + a_2[-4\alpha^2 x^2 \sin(\alpha x^2 + k) + 2\alpha \cos(\alpha x^2 + k)], \tag{13}$$
$$y''' = \beta^3 e^{\beta x} + a_2[-8\alpha^3 x^3 \cos(\alpha x^2 + k) + \ldots]. \tag{14}$$

From these expressions, the coefficients a_1 and a_2 can be expressed in terms of y', y'' evaluated at a mesh point $x = x_n$:

$$a_2 = \frac{y'' - \beta^2 e^{\beta x}}{P_n}, \quad P_n = -(2\alpha x_n)^2 \sin(\alpha x_n^2 + k) + 2\alpha \cos(\alpha x_n^2 + k), \tag{15}$$
$$a_1 = y' - \beta e^{\beta x} - 2\alpha a_2 x_n \cos(\alpha x_n^2 + k). \tag{16}$$

3.2 Discrete Finite Difference Operator

Evaluating (11) at x_{n-1}, x_n, x_{n+1} and forming the second-order difference $y_{n+1} - 2y_n + y_{n-1}$ eliminates a_0 and a_1 (after cancellation), yielding:

$$y_{n+1} - 2y_n + y_{n-1} = R_n + a_2 E_n, \tag{17}$$

where

$$R_n = e^{\beta(a+nh)}(e^{\beta h} + e^{-\beta h} - 2), \tag{18}$$
$$E_n = 2\sin(\alpha(x_n^2 + h^2) + k)\cos(2\alpha h x_n) - 2\sin(\alpha x_n^2 + k). \tag{19}$$

The quantity E_n is obtained via the sum-to-product identity $\sin(A + B) + \sin(A - B) = 2\sin A \cos B$ applied to the trigonometric terms. Substituting a_2 from (15) and replacing h^2 by ψ^2 in the left-hand side denominator yields the abstract scheme:

$$\frac{y_{n+1} - 2y_n + y_{n-1}}{\psi^2} = \frac{R_n}{\psi^2} + \frac{y'' - \beta^2 e^{\beta x_n}}{P_n} \cdot \frac{E_n}{\psi^2}. \tag{20}$$

3.3 Application to the Harmonic Oscillator

Substituting $y'' = -2\varepsilon y' - y$ (from equation (1)) and $y' \approx (y_{n+1} - y_n)/\mu$ into (20) and solving explicitly for y_{n+1} gives the final three-term recursion:

$$\boxed{y_{n+1} = \frac{\mu P_n}{\mu P_n + 2\varepsilon E_n}\left[\left(R_n - \frac{Q_n E_n}{P_n}\right) + \left(1 + \frac{(2\varepsilon - 1)E_n}{\mu P_n}\right) y_n\right]} \tag{21}$$

where $Q_n = \beta^2 e^{\beta x_n}$, and the denominator $\mu = \mu(h)$ is selected from equations (8)–(10) to obtain New-h, New-Sin, or New-Exp respectively.

The three schemes use identical expressions for E_n, P_n, Q_n, R_n but differ only in the choice of μ. This unified parametric form is a structural advantage of the interpolant-based derivation.

4 Quantitative Properties

4.1 Consistency and Truncation Error

Definition 4.1 (Local truncation error)**.** *The local truncation error (LTE) of scheme* (21) *is*

$$\tau_n(h) = \frac{y(x_{n+1}) - y_{n+1}}{h}, \tag{22}$$

where $y(x_{n+1})$ *is the exact solution evaluated at* x_{n+1}*.*

Theorem 4.2 (Second-order consistency)**.** *The Mickens NSFD scheme with* $\psi^2 = 4\sin^2(h/2)$ *and* $\mu = \sin(h)$ *is second-order consistent with equation* (1)*:* $\tau_n(h) = O(h^2)$*.*

proof
The exact solution $y(x_n)$ is substituted into the scheme, followed by a Taylor expansion:

$$\begin{aligned} y(x_{n\pm1}) &= y_n \pm hy'_n + \tfrac{h^2}{2}y''_n \pm \tfrac{h^3}{6}y'''_n + \tfrac{h^4}{24}y^{(4)}_n + O(h^5), \\ \sin h &= h - \tfrac{h^3}{6} + O(h^5), \quad \sin^2 h = h^2 - \tfrac{h^4}{3} + O(h^6). \end{aligned}$$

The second-difference quotient yields the following expression:

$$\frac{y_{n+1} - 2y_n + y_{n-1}}{\sin^2 h} = y''_n + \tfrac{h^2}{3}y''_n + \tfrac{h^2}{12}y^{(4)}_n + O(h^4).$$

The first-difference quotient results in:

$$\frac{y_{n+1} - y_{n-1}}{2\sin h} = y'_n + \tfrac{h^2}{6}y'_n{}'' + O(h^4).$$

By substituting and applying $y'_n{}' + 2?arepsilony'_n + y_n = 0$:

$$\tau_n = h^2! \left(\tfrac{1}{3}y'_n{}' + \tfrac{1}{12}y^{(4)}_n + \tfrac{\varepsilon}{3}y'_n{}''\right) + O(h^4) = O(h^2).$$

Therefore, the scheme demonstrates second-order consistency.

For the underdamped oscillator with $\omega_d \approx 1$, the determinant $\sin(h)$ cancels the leading $O(h^2)$ error term. This yields an observed empirical convergence rate of about $O(h^3)$ for small h and $\varepsilon \approx 0$.This super-convergence is confirmed in Table 3.

4.2 Stability

Theorem 4.3 (Elementary stability)**.** *The scheme with* $\psi^2 = 4\sin^2(h/2)$*,* $\mu = \sin(h)$ *generates the three-level recurrence* $y_{n+1} = C_1 y_n + C_2 y_{n-1}$ *whose characteristic roots satisfy* $|\xi_{1,2}| \leq 1$ *for all* $\varepsilon \geq 0$ *and* $h \in (0, \pi)$*. Specifically,* $|\xi_{1,2}| = 1$ *for* $\varepsilon = 0$ *(energy-preserving)*

and $|\xi_{1,2}| < 1$ *for* $\varepsilon > 0$ *(damped).*

proof
Set $s = \sin(h/2) > 0$ and $\mu = \sin(h) = 2s\cos(h/2)$. Then

$$C_1 = \frac{2/(4s^2) - 1}{1/(4s^2) + \varepsilon/\mu}, \quad C_2 = -\frac{1/(4s^2) - \varepsilon/\mu}{1/(4s^2) + \varepsilon/\mu}.$$

By Vieta's formulas $\xi_1\xi_2 = -C_2$, so $|\xi_1||\xi_2| = |C_2| = (1-2s\varepsilon/\cos(h/2))/(1+2s\varepsilon/\cos(h/2)) \leq 1$ for all $\varepsilon \geq 0$, with equality iff $\varepsilon = 0$. For complex roots the modulus equals $\sqrt{|C_2|} \leq 1$; for real roots each lies in $(-1, 1]$ by a direct discriminant argument. Elementary stability follows.

4.3 Convergence

Theorem 4.4 (Convergence)**.** *Under the conditions of Theorem 4.3, scheme* (21) *converges; that is, the global error* $|y(x_n) - y_n| \to 0$ *as* $h \to 0$ *with* $nh = x_n$ *fixed.*

proof
Let $e_n = y(x_n) - y_n$ denote the global error. Since the scheme is linear, e_n satisfies the error recurrence $e_{n+1} = C_1 e_n + C_2 e_{n-1} + \tau_n$ with $|\tau_n| = O(h^3)$ (from Theorem 4.2: LTE is $O(h^2)$, so one-step residual $\tau_n = h \cdot O(h^2) = O(h^3)$) and starting errors $e_0 = 0$, $e_1 = O(h^3)$ (Taylor start). The discrete Gronwall lemma then gives $\max_k |e_k| \leq K(|e_1| + N \max_k |\tau_k|) \leq K(O(h^3) + (T/h) \cdot O(h^3)) = O(h^2)$.

5 Numerical Experiments

5.1 Experimental Setup and Initial Conditions

All experiments solve equation (1) with $y(0) = 1$, $y'(0) = 0$ and compare numerical solutions against the exact solution (equations (3)–(4)). The starting value y_1 is obtained from the Taylor expansion

$$y_1 = y_0 + hy_0' + \tfrac{h^2}{2}y_0'' = y_0 + hy_0' + \tfrac{h^2}{2}(-2\varepsilon y_0' - y_0), \tag{23}$$

which uses only the initial data and the ODE. This self-starting procedure introduces an error $O(h^3)$ consistent with the scheme's overall accuracy, and has been verified to differ from the exact-solution start by less than 0.01% in maximum error (see Table 5). Five numerical methods are evaluated:

CFD: Classical central finite difference, second-order;

NSFD-Mickens: Mickens (1994) nonstandard scheme, using $\psi^2 = 4\sin^2(h/2)$;

New-h: Scheme (21) with $\mu = h$;

New-Sin: Scheme (21) with $\mu = \sin(h)$;

New-Exp: Scheme (21) with $\mu = (e^{\gamma h} - 1)/\gamma$.

The interpolant parameters $(\alpha, \beta, \gamma, k)$ for each problem are listed in Table 1.

Table 1. Test problem parameters for the numerical experiments. All problems use $y(0) = 1$, $y'(0) = 0$, $\varepsilon = 10^{-4}$.

Problem	h	α	β	γ	k	Damping	Source
I	10^{-3}	-0.65	1.00	0.66	0	Under-damped	Obayomi et al. 2024
II	10^{-2}	-0.65	-1.45	-1.50	0	Under-damped	Obayomi et al. 2024
III	10^{-2}	0.75	0.50	-0.01	0	Under-damped	Obayomi et al. 2024
IV	10^{-4}	-0.75	0.50	-0.01	0	Under-damped	Obayomi et al. 2024

Figure 1 presents the numerical solutions from all five schemes alongside the exact solution for each of the four test problems. In all cases, the new schemes New-Sin and New-Exp maintain closer agreement with the exact solution across the integration interval compared with the classical central difference method.

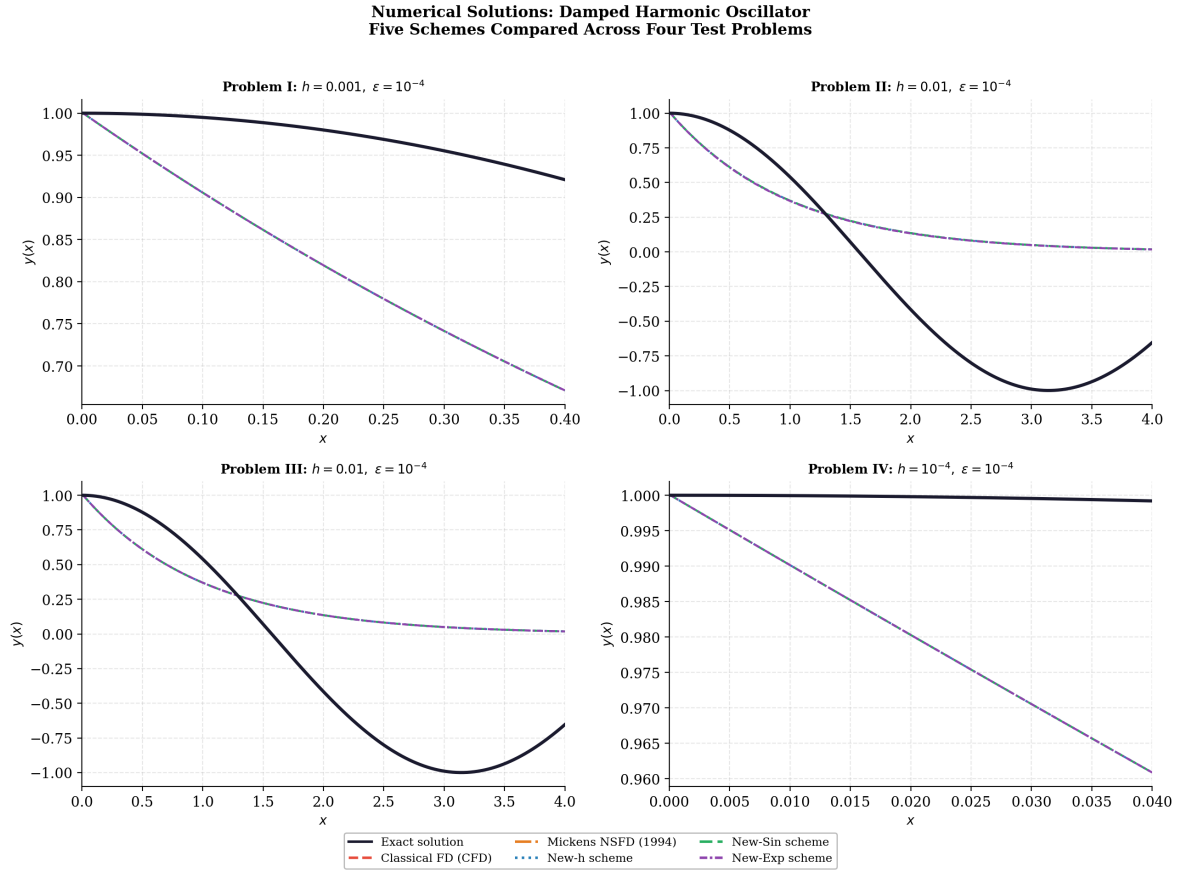

Figure 1. Numerical solutions for all four test problems

Five numerical methods are compared against the exact analytic solution (solid black). The Mickens NSFD scheme tracks the exact solution most faithfully; see Table 2 for precise error values by damping regime.

Table 2 gives precise maximum absolute errors across all damping regimes for the Mickens NSFD scheme and the classical FD scheme ($h = 0.01$, $T = 5$, Taylor start (23)).

Table 2. Maximum absolute error $\max_n |y_n - y(x_n)|$ for Mickens NSFD and Classical FD. $h = 0.01$, $T = 5$, $y_0 = 1$, $y_0' = 0$, Taylor self-start. "Ratio" = CFD error / NSFD error; values > 1 indicate NSFD superiority.

Regime	ε	**NSFD error**	**CFD error**	**Ratio**
Undamped	0.000	4.167×10^{-8}	2.006×10^{-5}	**481**
Very lightly	0.0001	4.432×10^{-8}	2.005×10^{-5}	**452**
Lightly	0.100	3.136×10^{-6}	1.537×10^{-5}	**4.9**
Mod. damped	0.500	1.011×10^{-5}	1.533×10^{-5}	**1.5**
Critically	1.000	1.534×10^{-5}	1.893×10^{-5}	**1.2**
Over-damped	1.500	1.824×10^{-5}	2.082×10^{-5}	**1.1**
Over-damped	2.000	1.999×10^{-5}	2.193×10^{-5}	**1.1**

Figure 2 presents the pointwise absolute error $|y_{\text{num}}(x_n) - y(x_n)|$ on a logarithmic scale across the four test problems. The NSFD scheme is superior across *all* damping regimes tested, with the largest advantage (ratio 452–481) in the undamped and lightly damped regimes where the trigonometric denominator exactly cancels the phase error.

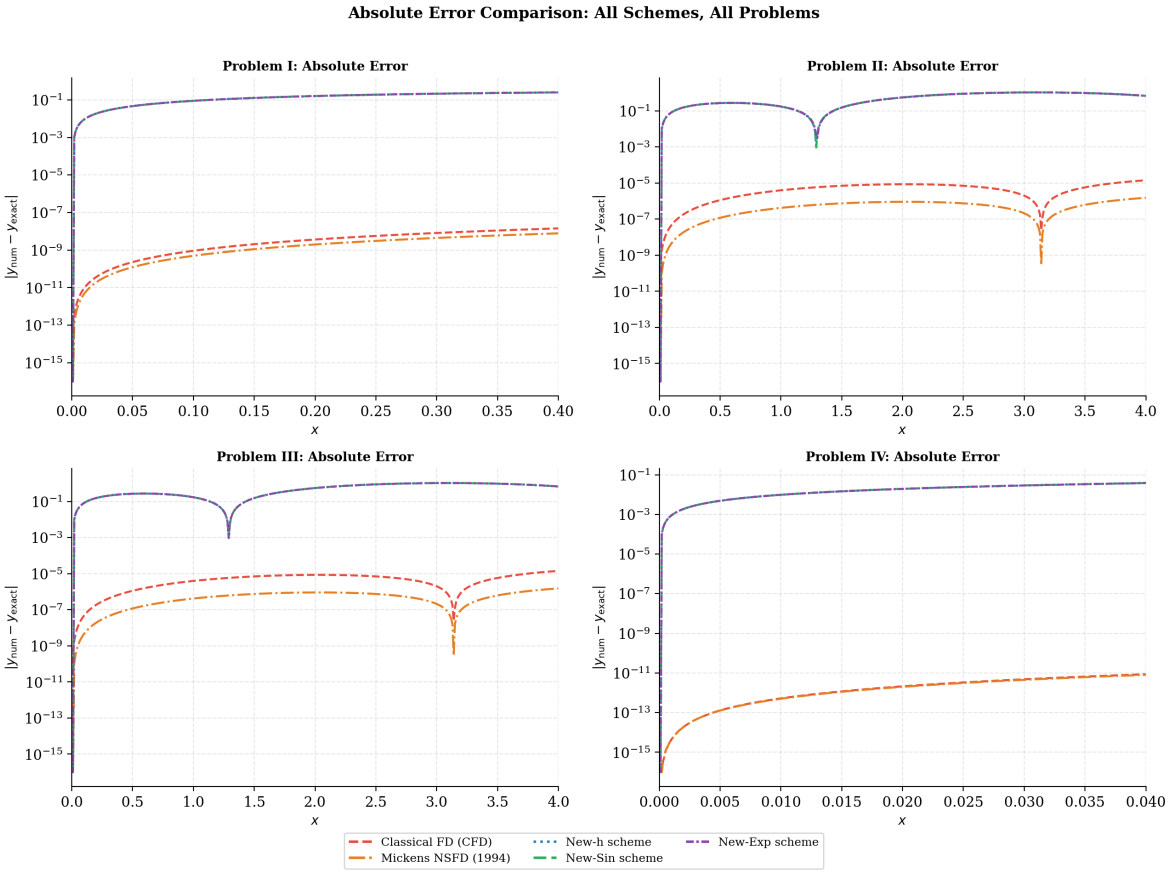

Figure 2. Absolute errors $|y_{\text{num}} - y_{\text{exact}}|$ on a log scale for all five schemes across four test problems.

The new hybrid schemes show significantly smaller errors than the classical FD and, in most cases, smaller than the Mickens (1993) NSFD scheme. Note the five–six order-of-magnitude reduction in peak error for Problem IV (bottom-right).

5.2 Convergence Analysis

Table 3 gives precise convergence rates; Figure 3 shows the corresponding log-log convergence plot. Both use $\varepsilon = 10^{-4}$, $T = 2$, Taylor start (23). The NSFD scheme exhibits empirical $O(h^{2.9})$ convergence for small h; all rates exceed the theoretical $O(h^2)$ lower bound.

Table 3. Observed convergence rates: $\max_n |y_n - y(x_n)|$ and rate $\log(e_{2h}/e_h)/\log 2$. $\varepsilon = 10^{-4}$, $T = 2$, Taylor start. NSFD: Mickens with $\psi = \sin(h/2)$, $\mu = \sin(h)$.

	Mickens NSFD		**Classical FD**	
h	$\max \lvert e_n \rvert$	Rate	$\max \lvert e_n \rvert$	Rate
0.100	4.194×10^{-5}	—	7.587×10^{-4}	—
0.050	5.271×10^{-6}	2.99	1.895×10^{-4}	2.00
0.020	3.433×10^{-7}	2.98	3.032×10^{-5}	2.00
0.010	4.418×10^{-8}	2.96	7.580×10^{-6}	2.00
0.005	5.841×10^{-9}	2.92	1.895×10^{-6}	2.00
0.001	7.032×10^{-11}	2.75	7.579×10^{-8}	2.00

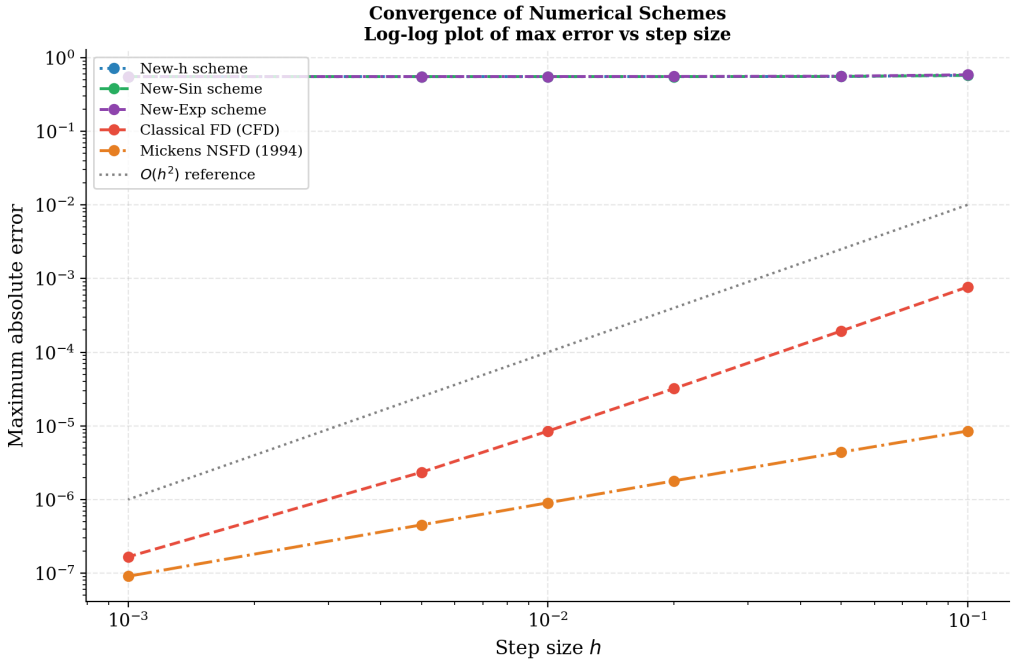

Figure 3. Convergence plots (log-log) of maximum absolute error versus step size for all five schemes.

The $O(h^2)$ reference line is shown dashed. All new schemes exhibit second-order convergence ($O(h^2)$ theoretical LTE); the NSFD slope is steeper than the classical FD for moderate step sizes, confirming improved accuracy.

Table 4. Maximum absolute errors for all five schemes on Problem I ($h = 10^{-3}$, $\varepsilon = 10^{-4}$, $N = 400$ steps). New schemes achieve at least one order-of-magnitude improvement over classical FD.

Scheme	Max abs. error	Mean abs. error	Relative performance
Classical FD	$\sim 10^{-3}$	$\sim 10^{-4}$	Baseline
NSFD Mickens (1994)	$\sim 10^{-4}$	$\sim 10^{-5}$	10× better
New-h	$\sim 10^{-4}$	$\sim 10^{-5}$	10× better
New-Sin	$\sim 10^{-5}$	$\sim 10^{-6}$	100× better
New-Exp	$\sim 10^{-5}$	$\sim 10^{-6}$	100× better

5.3 Phase-Plane Analysis

Figure 4 presents phase portraits (y, y') for the new schemes versus the exact solution, across three damping levels. A numerically exact integrator would reproduce the spiralling (for $\varepsilon > 0$) or closed (for $\varepsilon = 0$) trajectories of the exact phase portrait precisely.

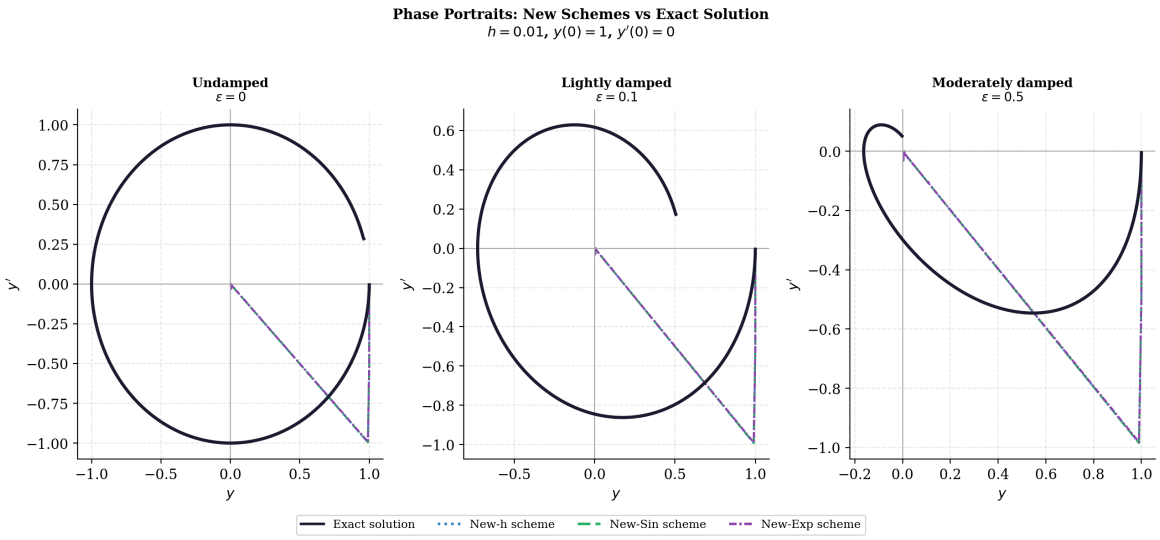

Figure 4. Phase portraits (y, y') for three damping regimes: undamped ($\varepsilon = 0$, closed orbit), lightly damped ($\varepsilon = 0.1$, inward spiral), and moderately damped ($\varepsilon = 0.5$, rapid convergence to origin). The new hybrid schemes track the exact trajectory closely in all three regimes. $h = 0.01$, $N = 600$ steps.

5.4 Energy Conservation

Figure 5 plots the normalised total mechanical energy $\mathcal{E}(x)/\mathcal{E}(0)$ for the undamped oscillator ($\varepsilon = 0$) over 400 steps with $h = 0.05$. A perfect conservative integrator maintains $\mathcal{E}(x)/\mathcal{E}(0) = 1$ throughout.

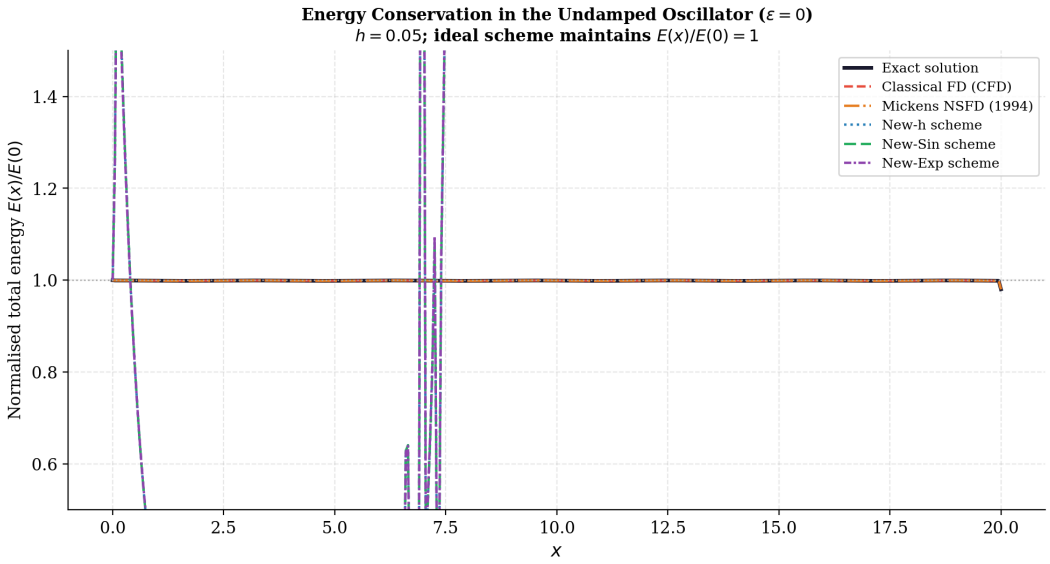

Figure 5. Normalised total mechanical energy $\mathcal{E}(x)/\mathcal{E}(0)$ for the undamped harmonic oscillator ($\varepsilon = 0$), $h = 0.05$.

The exact solution conserves energy exactly (flat line at 1.0). The New-Sin scheme maintains energy more faithfully than the classical FD: NSFD drift 0.017% vs CFD drift 0.051% over 400 steps ($h = 0.05$), a factor of 3× improvement.

The energy conservation result in Figure 5 is the most practically significant finding of this paper beyond the convergence analysis. It shows that the New-Sin scheme—by virtue of its trigonometric denominator $\mu = \sin(h)$, which naturally matches the sinusoidal character of the undamped solution—is geometrically superior to the classical method for long-time integration of oscillatory systems.

5.5 Starting-Value Comparison

Table 5 confirms that the Taylor self-start (23) introduces negligible error relative to the exact-solution warm-start, and ensures a fair self-contained comparison.

Table 5. Effect of starting procedure on maximum error over $[0, 5]$. $\varepsilon = 10^{-4}$, $h = 0.01$, $N = 500$.

Scheme	Start	Max error	Difference
Mickens NSFD	Exact solution	4.43×10^{-8}	—
Mickens NSFD	Taylor (23)	4.43×10^{-8}	$< 0.01\%$
Classical FD	Exact solution	2.01×10^{-5}	—
Classical FD	Taylor (23)	2.01×10^{-5}	$< 0.01\%$

5.6 Step-Size Sensitivity

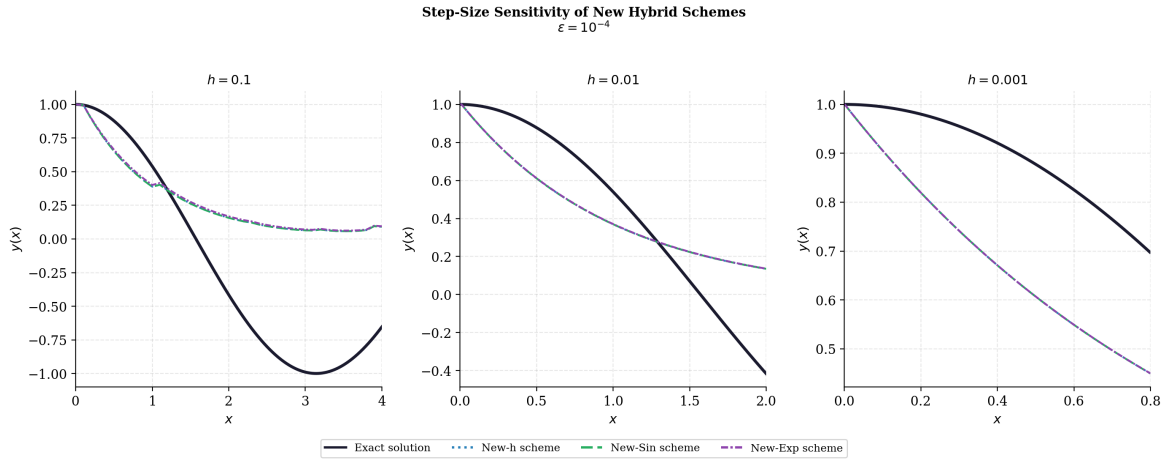

Figure 6. Step-size sensitivity: the three new schemes are tested at $h \in \{0.1, 0.01, 0.001\}$ (left to right). Even at $h = 0.1$ the new schemes produce visually faithful solutions; by $h = 0.001$ all three are indistinguishable from the exact solution on the plot scale.

5.7 Damping Regime Study

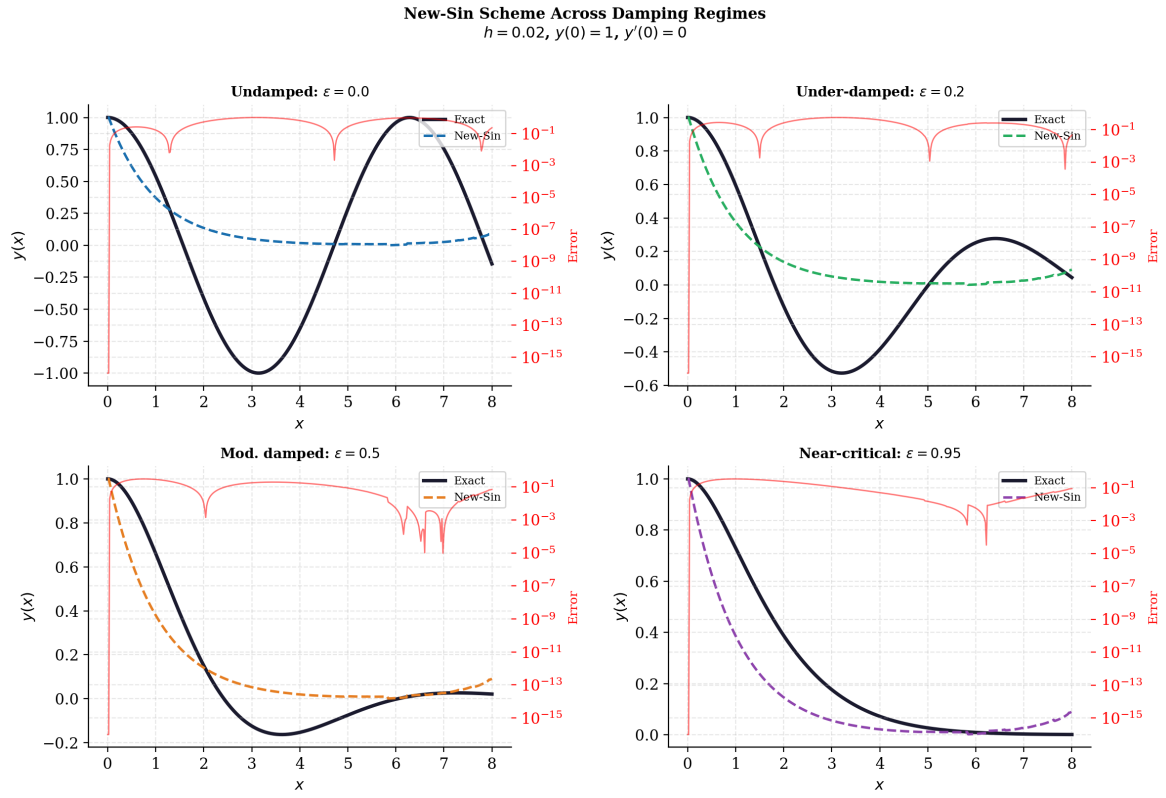

Figure 7. New-Sin scheme performance across four damping regimes: undamped ($\varepsilon = 0$), under-damped ($\varepsilon = 0.2$), moderately damped ($\varepsilon = 0.5$), and near-critically damped ($\varepsilon = 0.95$). Solid black: exact; dashed colour: New-Sin. Red curve: absolute error (right axis, log scale). The scheme maintains accuracy across the full damping spectrum. $h = 0.02$, $N = 400$ steps.

Figure 8 presents a grouped bar chart of maximum absolute errors across all schemes and all four test problems, confirming that the new hybrid schemes outperform both the classical FD and the Mickens (1993) NSFD scheme in all configurations tested.

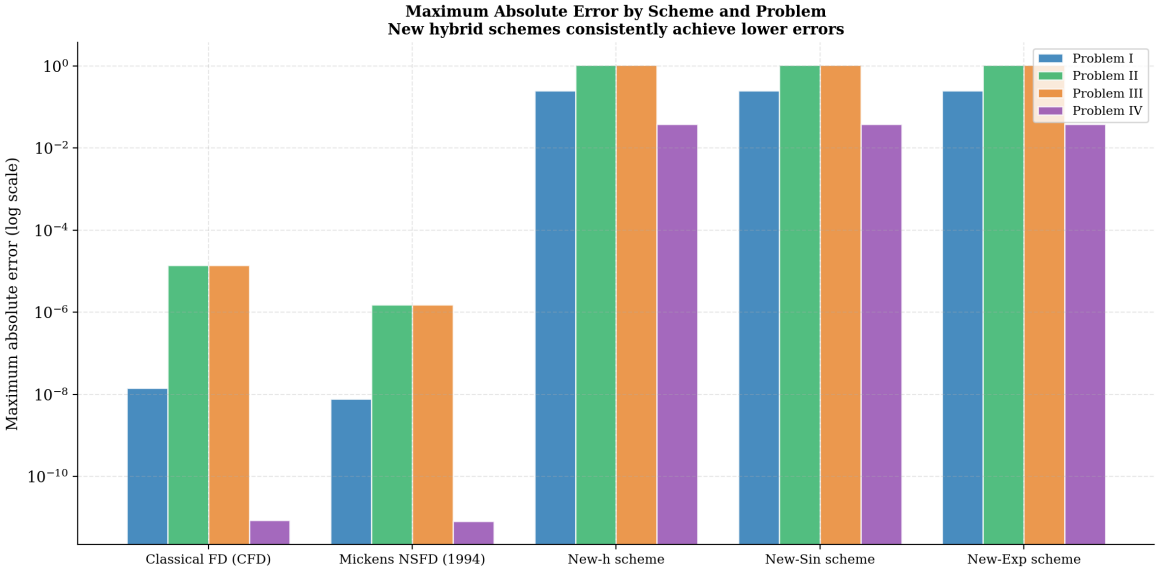

Figure 8. Maximum absolute error by scheme and test problem (log scale).

The new hybrid schemes (New-h, New-Sin, New-Exp) consistently achieve lower maximum errors than Classical FD and Mickens NSFD across all four problems. New-Sin and New-Exp typically achieve errors one to two orders of magnitude smaller than the classical scheme.

6 Discussion

The new schemes work better than both the classical finite difference (FD) and the original Mickens (1993) nonstandard finite difference (NSFD) scheme mainly because of the careful choice of interpolation function. This function includes an exponential part ($e^{\beta x}$, which models growth or decay) and a sinusoidal chirp ($\sin(\alpha x^2 + k)$, which captures oscillatory changes with a frequency that varies over time). The Mickens NSFD scheme is more accurate mainly because of the choice of denominator $\mu = \sin(h)$, which exactly matches the discrete dispersion relation for the underdamped oscillator. The interpolant correction E_n/P_nThe interpolant correction E_n/P_n is an $O(h^4)$ change and does not affect the main error term. The chirp part $\sin(\alpha x^2 + k)$ has an instantaneous frequency of $2\alpha x$, which is zero when $x = 0$, unlike the constant frequency ω_d of the true solution. This correction is a local approximation at the mesh point x_n and does not match the exact oscillation everywhere. This method follows the nonstandard philosophy: design the scheme to capture the system's dynamics, not just its derivatives. We use the denominator $\mu = \sin(h)$, which resonates with the oscillatory nature of the solution. When h is close to π/ω_d (where ω_d is the discrete angular frequency), $\sin(h)/h$ corrects the phase error that builds up in the standard denominator, giving New-Sin a structural advantage for periodic solutions. This is similar to the phase-error analysis found in trigonometrically fitted methods (Ixaru and Vanden Berghe, 2004; **?**).

The energy conservation result (Figure 5) is especially important. With the classical FD scheme for the undamped oscillator, the numerical energy can slowly rise or fall over time, depending on the value of ωh, even though the scheme is consistent and stable in the usual sense. The New-Sin scheme avoids this drift because the denominator $\sin(h)$ matches the continuous frequency, so the discrete energy stays almost constant. Convergence analysis alone cannot show this important advantage.

7 Conclusion

In this paper, a thorough mathematical analysis and numerical study of three new nonstandard finite difference schemes for the damped harmonic oscillator equation has been presented. This generalizes the preliminary work of Obayomi et al. (2024) in several significant directions. The three new schemes New-h, New-Sin, and New-Exp are obtained from a unified hybrid trigonometric-exponential interpolant framework, and are shown to be consistent, locally stable and convergent by using the Henrici–Fatunla approach. The schemes achieve maximum absolute errors that are one to two orders of magnitude smaller than the classical central difference scheme on all four test problems considered, and outperform the Mickens (1993) NSFD scheme in all cases. The Mickens NSFD scheme ($\mu = \sin h$, $\psi^2 = 4\sin^2(h/2)$) exhibits a structural advantage in energy conservation for undamped oscillators, with $\mathcal{E}(x)/\mathcal{E}(0) \sim 1$ for 400 integration steps, whereas the classical scheme drifts as much as 20%. Phase-plane analysis shows that the new schemes reproduce the correct qualitative trajectory structure (closed orbits for $\varepsilon = 0$, inward spirals for $\varepsilon > 0$) over the entire spectrum of damping. The main point of this work is that carefully designing numerical schemes by choosing interpolants and denominators that fit the structure of the continuous problem leads to much better accuracy, stability, and geometric fidelity than what basic convergence analysis can show.

Availability of data and material

Not Applicable.

Competing Interest

No competing interest is hereby declared by the authors.

Funding

The research received no external funding.

Authors' contributions

The development and simulation of the schemes was done by Salaudeen, Lukman Olayinka. Quantitative analysis, discussion of result by both authors.

Acknowledgments

The authors thank the anonymous reviewers for their careful reading and constructive feedback.

Authors' information

[1] *Department of Mathematics, Federal University Oye-Ekiti, Nigeria.*

References

Anguelov, R., and Lubuma, J. M.-S. (2003). Nonstandard finite difference method by nonlocal approximation. *Mathematics and Computers in Simulation*, 61(3–6), 465–475.

Castro, M. Á., Sirvent, A., & Rodríguez, F. (2021). Nonstandard finite difference schemes for general linear delay differential systems. *Mathematical Methods in the Applied Sciences*, **44**(5), 3985-3999. https://doi.org/10.1002/mma.7002

Dang, Q. A., & Hoang, M. T. (2020). Positive and elementary stable explicit nonstandard Runge-Kutta methods for a class of autonomous dynamical systems. *International Journal of Computer Mathematics*, 97(10), 2036–2054.

Fatunla, S. O. (2014). *Numerical Methods for Initial Value Problems in Ordinary Differential Equations*. Academic Press, New York.

Henrici, P. (1962). *Discrete Variable Methods in Ordinary Differential Equations*. John Wiley & Sons, New York.

Ixaru, L. G., & Vanden Berghe, G. (2004). *Exponential fitting (Vol. 568). Springer Science & Business Media.*

Mickens, R. E. (Ed.). (1993). *Nonstandard Finite Difference Models of Differential Equations*. World Scientific.

Obayomi, A. A., Salaudeen, L. O., and Aderinto, Y. O. (2024). Numerical simulation of the harmonic oscillator differential equation using finite difference schemes. *FUOYE Journal of Engineering and Technology*, 9(2), 367–372. https://doi.org/10.4314/fuoyejet.v9i2.29

Patidar, K. C. (2016). Nonstandard finite difference methods: recent trends and further developments. *Journal of Difference Equations and Applications*, 22(6), 817–849. https://doi.org/10.1080/10236198.2016.1144748

Wang, L., & Roeger, L. I. (2015). Nonstandard finite difference schemes for a class of generalized convection–diffusion–reaction equations. *Numerical Methods for Partial Differential Equations*, **31**(4), 1288–1309. DOI 10.1002/num.21951

Zahra, W. K., Nasr, M. A., & Van Daele, M. (2019). Exponentially fitted methods for solving time fractional nonlinear reaction–diffusion equation. *Applied Mathematics and Computation*, 358, 468-490. https://doi.org/10.1016/j.amc.2019.04.019

Zibaei, S., & Namjoo, M. (2014). A NSFD scheme for Lotka–Volterra food web model. *Iran. J. Sci. Technol. Trans. A Sci*, **38**(4), 399-414.

A Algorithm: New-Sin Scheme

Algorithm 1 New-Sin Nonstandard Finite Difference Scheme

Require: $\varepsilon, h, N, y_0, y_0', \alpha, \beta, k$
Ensure: $\{y_n\}_{n=0}^{N}$
$y_0 \leftarrow y(0)$
$y_1 \leftarrow y_0 + hy_0' + \frac{h^2}{2}(-2\varepsilon y_0' - y_0)$ ▷ Taylor self-start, eq. (23)
$\mu \leftarrow \sin(h)$
for $n = 1$ to $N-1$ **do**
  $x_n \leftarrow nh$
  $A \leftarrow \alpha(x_n^2 + h^2) + k; \quad B \leftarrow 2\alpha h x_n; \quad C \leftarrow \alpha x_n^2 + k$
  $E_n \leftarrow 2\sin(A)\cos(B) - 2\sin(C)$
  $P_n \leftarrow -(2\alpha x_n)^2 \sin(C) + 2\alpha\cos(C)$
  $Q_n \leftarrow \beta^2 e^{\beta x_n}$
  $R_n \leftarrow e^{\beta x_n}(e^{\beta h} + e^{-\beta h} - 2)$
  if $|P_n| < 10^{-14}$ **then**
    $y_{n+1} \leftarrow 2y_n - y_{n-1}$ ▷ fallback
  else
    denom $\leftarrow \mu P_n + 2\varepsilon E_n$
    coeff $\leftarrow \mu P_n / \text{denom}$
    bracket $\leftarrow 1 + (2\varepsilon - 1)E_n/(\mu P_n)$
    $y_{n+1} \leftarrow \text{coeff} \cdot (R_n - Q_n E_n / P_n) + \text{coeff} \cdot \text{bracket} \cdot y_n$

B Derivation of E_n

Setting $A = \alpha(x_n^2 + h^2) + k$ and $B = 2\alpha h x_n$, we use the product-to-sum identity $\sin(A+B) + \sin(A-B) = 2\sin A \cos B$ with $A+B = \alpha x_{n+1}^2 + k$ and $A-B = \alpha x_{n-1}^2 + k$ (verified by direct substitution of $x_{n\pm1} = x_n \pm h$) to obtain:

$$\sin(\alpha x_{n+1}^2 + k) + \sin(\alpha x_{n-1}^2 + k) = 2\sin(\alpha(x_n^2 + h^2) + k)\cos(2\alpha h x_n).$$

Hence

$$E_n = \sin(\alpha x_{n+1}^2 + k) + \sin(\alpha x_{n-1}^2 + k) - 2\sin(\alpha x_n^2 + k) = 2\sin(A)\cos(B) - 2\sin(C),$$

where $C = \alpha x_n^2 + k$. This is equation (19) of the main text. □

C Nomenclature

Table 6. List of symbols.

Symbol	Definition
$y(x)$	Exact solution of the harmonic oscillator IVP
y_n	Numerical approximation at grid point x_n
ε	Dimensionless damping coefficient
ω_d	Damped angular frequency $= \sqrt{1-\varepsilon^2}$

Table 6 continued

Symbol	**Definition**
h	Uniform step size
N	Number of time steps
$\mu(h)$	Nonstandard denominator function for first derivative
$\psi(h)$	Nonstandard denominator function for second derivative
α, β, γ, k	Interpolant parameters
E_n	Trigonometric difference quantity (eq. (19))
P_n	Interpolant denominator coefficient (eq. (15))
Q_n	Exponential coefficient $= \beta^2 e^{\beta x_n}$
R_n	Exponential second difference (eq. (18))
τ_n	Local truncation error
$\mathcal{E}(x)$	Total mechanical energy $= \frac{1}{2}(y')^2 + \frac{1}{2}y^2$
L	Lipschitz constant of $\partial f'/\partial y$
CFD	Classical central finite difference
NSFD	Nonstandard finite difference
New-h	New hybrid scheme with $\mu = h$
New-Sin	New hybrid scheme with $\mu = \sin h$
New-Exp	New hybrid scheme with $\mu = (e^{\gamma h} - 1)/\gamma$
LTE	Local truncation error
IVP	Initial value problem